ELSEVIER

Radiotherapy and Oncology 45 (1997) 263–269

RADIOTHERAPY & ONCOLOGY
JOURNAL OF THE EUROPEAN SOCIETY FOR THERAPEUTIC RADIOLOGY AND ONCOLOGY

Transfer of information between angiographic films and CT images: a technique to control the drawing of target volumes

Pierre-Alain Tercier[a,*], Philippe Coucke[b], Heinz Fankhauser[c], René-Olivier Mirimanoff[b], Antoine Uské[d], Jean-François Valley[a]

[a]*Institute of Applied Radiophysics, University Center, CH-1015 Lausanne, Switzerland*
[b]*Department of Radiooncology, CHUV, CH-1005 Lausanne, Switzerland*
[c]*Department of Neurosurgery, CHUV, CH-1005 Lausanne, Switzerland*
[d]*Department of Radiodiagnostics, CHUV, CH-1005 Lausanne, Switzerland*

Received 21 January 1997; revised version received 1 July 1997; accepted 10 July 1997

Abstract

Background and purpose: This work was undertaken to improve the definition of target volumes for radiosurgery using the angiographic and CT data.

Materials and methods: The basis of this new method is to combine both imaging modalities and to compare them in each representation, i.e. to plot the volume obtained by angiography on CT images and also the contours defined by the CT on angiographic films. To obtain the angiographic volume, the radiographs are taken at several incidence angles. The X-ray sources position and the position of the films are determined using rectangular markers, then the intersection of all the loci of the target volume are calculated.

Results: Verifications with a phantom show the accuracy of the procedure and the benefit obtained by increasing the number of angles of incidence in the angiographic imaging. The centre of gravity of the experimental target could be localized to an accuracy of better than 0.4 mm. The method was used in 11 clinical cases with excellent clinical results.

Conclusions: The method can be easily applied and improves the delineation of target volumes in radiosurgery. CT data counterbalances the relative weakness of angiography concerning the three-dimensional geometry. Angiography adds useful information on the blood flow that is not shown in CT. Almost all the presented clinical cases benefit from the technique described here. © 1997 Elsevier Science Ireland Ltd.

Keywords: Radiosurgery; Angiography; Stereotaxy; Arterio-venous malformations; Multimodality imaging

1. Introduction

Stereotactic radiotherapy and single fraction radiosurgery have a long history [12,13]. However, it is only with its implementation on linear accelerators that the use of this high precision technique has become more widespread [8,9].

One major indication for single fraction radiosurgery is patients with small-sized unresectable arteriovenous malformations (AVM). This procedure requires adequate localization of the nidus with suitable high precision imaging techniques. In order to obtain a reliable delineation of the target volume, we aim to combine data from different radiological techniques, i.e. computer tomography (CT) and angiography. For arteriovenous malformations the angiography yields supplementary information on arterial and venous sides of the lesion, whereas the CT data allow an improved spatial delineation of the nidus. In order to combine information obtained by the two techniques and to check the accuracy of nidus localization with each technique, we have developed a method to match the two locations and hence to monitor the drawing of the target volume.

The aim is to define the position of the lesion in the patient with a stereotactic ring (or frame) fixed to the patient's head defining the reference stereotactic co-ordi-

* Corresponding author.

PII S0167-8140(97)00140-0

nate system. Angiography is used to localize the lesion on sets of films. To obtain the three-dimensional co-ordinates necessary for the treatment, reference markers must be attached to the ring and appear on the radiographs. Various methods exist and are well documented. Some of these systems [10] employ a long distance between the focus and the radiographs, avoiding the problem of divergence. Bergström et al. [1] retrieve the co-ordinates of a point by means of a graphical method, using square graduated reference marks projected on two films taken at short distances. Siddon and Barth [17] required only four rectangular markers attached to the ring in order to find the co-ordinates of the centre of the lesion by means of two independent radiographs. These films are not required to be parallel to the marker planes, in contrast to other systems [2,15] and also the incidence of the films do not need to be orthogonal. Using this method, the required conditions are simple; on each short distance radiograph, only the lesion and two rectangular markers need to be identified. Siddon and Barth's method is highly accurate, however, it does not describe the extension and shape of a non-ellipsoidal target.

With the objective of improving diagnostic accuracy, many authors [4,16,21] combine different imaging modalities such as CT, MRI and PET. In the case of AVMs, angiography provides further information, allowing the nidus and the arterial and venous sides of a lesion to be distinguished. According to some authors [3], systematic errors can occur when the determination of the target volume is based only on angiography. Others [18] point out that CT with a contrast agent can, in some circumstances, give an improved spatial definition of the nidus. However, clips or embolization material in the brain can produce artefacts on CT images. It is, therefore, important to be able to compare both imaging methods for each patient. In order to combine these two modalities, it is possible to project the voxels of the CT examination on to the angiography films. This is done using digital reconstructed radiographs (DRR), using the density of the voxels of the CT [7,14]. The matching of the two images is obtained by an iterative procedure. It minimizes the discrepancy between the real film and the DRR by searching for the right positions of the reconstructed film and X-ray source in a series of small steps. A second method, incorporating the angiographic information in the CT slices, allows the direct use of the combined diagnostics for the radiotherapy treatment planning on CT images. Foroni et al. [6] work in this direction. Their method is based on two angiographic series (front and lateral) and presupposes that the intersection of the lesion with each CT slice is elliptic.

The subject of this paper is to generalize the approach. The method described here is based on the same theory as Siddon and Barth [17]. The new concepts are a precise reconstruction of the volume defined by angiography and a direct comparison with CT without presuppositions concerning the shape of the lesion. Our method permits also the use of more than two incidences for the angiographic examination, improving the results in case of complex lesion.

In case of angiography the shape of the target volume is determined by two or more independent films taken at short distances. The projection of graduated scales is not necessary. The calculations take into account four rectangular markers fixed to the stereotactic ring. The algorithm calculates the position of the focus and the film in terms of the coordinate system of the ring. The outlined lesion on the film determines a conic locus of the target volume. This way, one obtains not only the co-ordinates of the centre of the lesion, but also the volume resulting from the intersection of the cones corresponding to all the radiographs. Finally, the treatment planning system superimposes the contours of the volume defined by angiography on the CT slices. Conversely the contour drawn by the medical doctor on CT slices is represented on angiographic films.

This paper describes a technique for the registration of CT and angiographic images. A report of the methods and clinical usage is followed by a presentation of results concerning the precision. A summarized report of some clinical cases and a detailed case study illustrate the application.

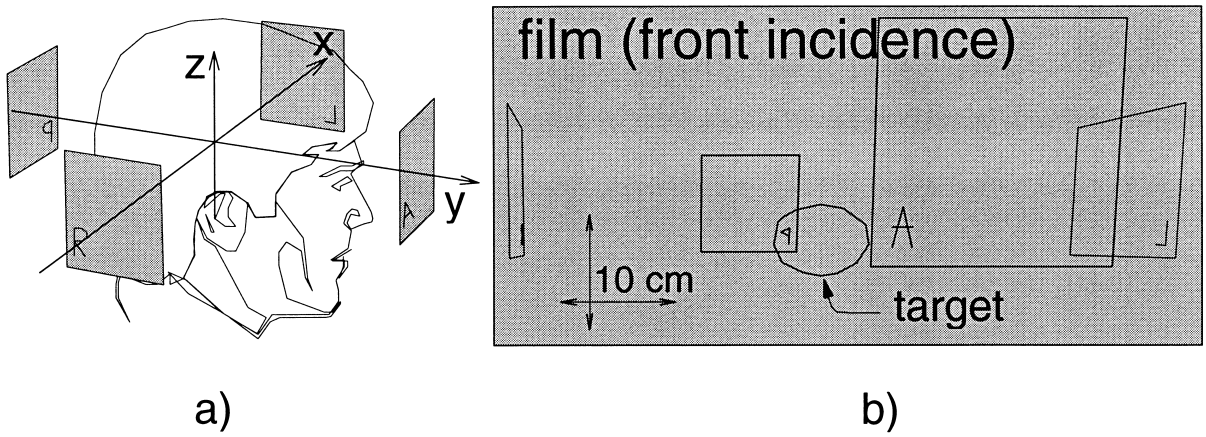

Fig. 1. Basic data. (a) Angiographic reference marks; (b) radiograph of the reference marks (in this case anterior and posterior) and the target.

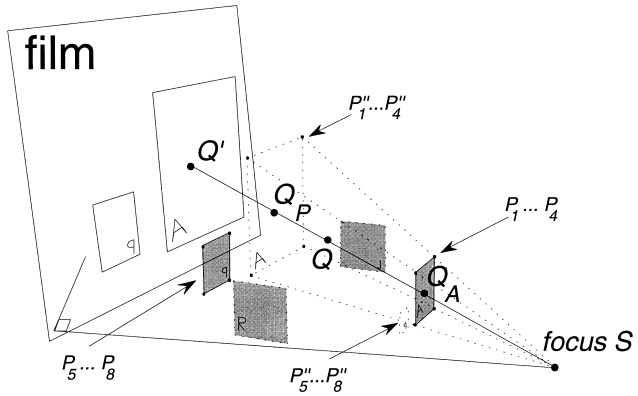

Fig. 2. Ignoring the position of Q, it is possible to find Q_A and Q_P knowing Q'. The lines $P_iP''_i$ converge to the X-ray focus S.

2. Materials and methods

2.1. Theory

2.1.1. Principles

A stereotactic ring or frame (which defines the reference co-ordinate system), is fixed to the patient's skull. Rectangular markers of radio-opaque wires are attached to the ring and radiographs of the system are taken using any incidence angle (see Fig. 1). Based on the outline of the lesion and the projection of two rectangular reference marks, a three-dimensional locus of the target volume is reconstructed.

The method used is based on the Pappus theorem [20] and the development by Siddon and Barth [17]. The Siddon and Barth results could be summarized as follow. Consider a point Q and an X-ray focus S in space. S lights Q and projects the image of Q onto the radiograph at Q' (see Fig. 2). Taking into account only the film in two dimensions (i.e. without knowledge of the location of the focus) and from the projection Q' of Q, the intersections of the straight line SQ' with the anterior (Q_A) and posterior (Q_P) reference mark planes can be calculated. Under these conditions, the enlarging ratios M_A and M_P, are defined by:

$$M_A = \frac{SQ'}{SQ_A},\ M_P = \frac{SQ'}{SQ_P} \tag{1}$$

Based on this method Siddon and Barth obtain the position of the centre of the lesion intersecting the lines (Q_A-Q_P) of the front view and (Q_L-Q_R) of the lateral view. The extend of the lesion is approximated using enlarging ratios. The exact shape of the lesion is not accessible. To avoid this deadlock a new idea was applied, i.e. instead of directly finding the lesion, we localize the X-ray focus (Section 2.1.2) then the film position (Section 2.1.3) and finally a locus of the lesion (Section 2.1.4). The procedure is repeated for each incidence and the intersection of all the loci gives the final volume (Section 2.1.4).

2.1.2. Focus localization

Using the method of Siddon and Barth [17], it is possible to construct the intersections ($P''_1,\ldots,P''_4$) of the lines going from the focus to the corners of the anterior marker ($P_1,\ldots,P_4$) on the film ($P'_1,\ldots,P'_4$) with the plane of the posterior marker (see Fig. 2). Put in the same words as the first part of the legend of Fig. 2, that gives: 'ignoring the position of ($P_1,\ldots,P_4$), it is possible to find ($P''_1,\ldots,P''_4$) knowing the corresponding points ($P'_1,\ldots,P'_4$) on the film'. The same can be done for the posterior marker ($P_5,\ldots,P_8$) finding ($P''_5,\ldots,P''_8$) in the plane of the anterior marker.

These eight reconstructed points (P''_i) and their corresponding real points (P_i) define eight lines in space, which converge at the unknown X-ray focus spot S. The set of linear equations (Eq. (2)), giving the solution S, is overdetermined and the result is obtained by a non-iterative least-squares method.

$$\begin{cases} S_x = k_i \cdot d_{i_x} + P_{i_x} \\ S_y = k_i \cdot d_{i_y} + P_{i_y},\ i = 1\ldots8 \\ S_z = k_i \cdot d_{i_z} + P_{i_z} \end{cases} \tag{2}$$

where $\vec{P}_i, (i=1\ldots8)$, describes the reference mark points, the k_i are the free parameters, the $\vec{d}_i$ are the line vectors and $k_i \cdot \vec{d}_i + \vec{P}_i$ describe the lines in space.

2.1.3. Localization of the radiographic plane

The local magnification ratios (M_i) of each point (P_i) of the anterior and posterior markers are calculated from Eq. (1) as explained in Ref. [17]. The position of the X-ray source is known from Eq. (2) and using Eq. (3), the position of each projected point (F_i) is determined. All these points (F_i) are in the film plane:

$$\vec{F}_i = \vec{S} + M_i \cdot \left(\vec{P}_i - \vec{S};\right) \tag{3}$$

A non-iterative least-squares method is used to determine this plane. It is to be noted that each point (F_i) correspond to a point (P'_i). They are not equal. The difference is that each point (P'_i) is measured on the film (2D) and the points (F_i) are placed in the space (3D).

2.1.4. Locus of the target volume and integration into the CT slices

To obtain a locus of the target volume defined by one

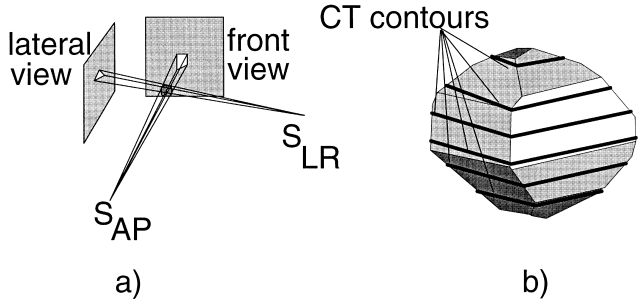

Fig. 3. The intersection of the cones (a) determines the angiographic target volume arranged slice by slice in the CT images (b). The co-ordinate system is aligned by CT and angiography guide marks.

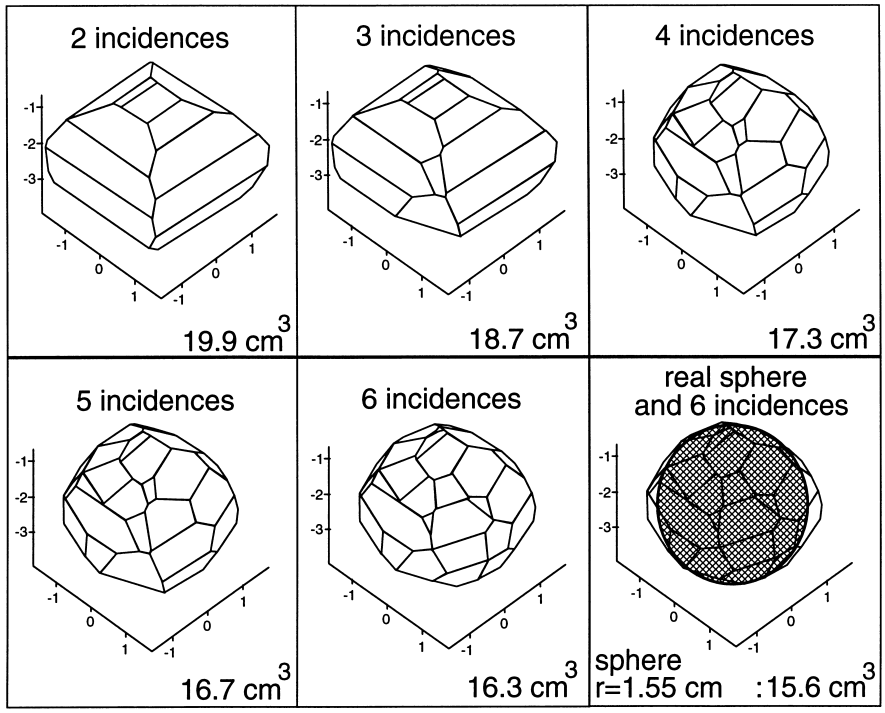

Fig. 4. Three-dimensional views of the reconstructed sphere. The calculated target volume in cubic centimetres is represented for each case.

radiograph a cone is constructed with the target volume outline from the film as the base and the vertex being the X-ray focus (see Fig. 3a). The X-ray source and image plane positions are found using the same algorithm for all incidence angles. In other words, such a cone exists for each radiograph and the intersection of all the loci constitutes the final volume given by contiguous facets. The contours of the angiographic volume in the CT slices are then obtained by cutting this volume with the CT planes (see Fig. 3b). These contours are displayed by the treatment planning system on the CT images to be compared with the contours previously drawn by the medical doctor.

2.1.5. Topological constraints

Non-convex volumes cannot always be completely reconstructed by this method. For example, a shape with an invaginated part cannot be taken into account with two incidences. Other non-convex volumes with an extremum of the saddle type (as found in a banana shape) are manageable, even if they necessitate the creation of two (or more) disjointed contours to be represented in the CT sections. With more than two incidences, assuming that each part of the lesion can be identified on the angiography, the problem of invaginated lesion can be solved by treating the lesion as a combination of convex sub-volumes. The classical coin problem [3,5,18] where the thickness cannot be

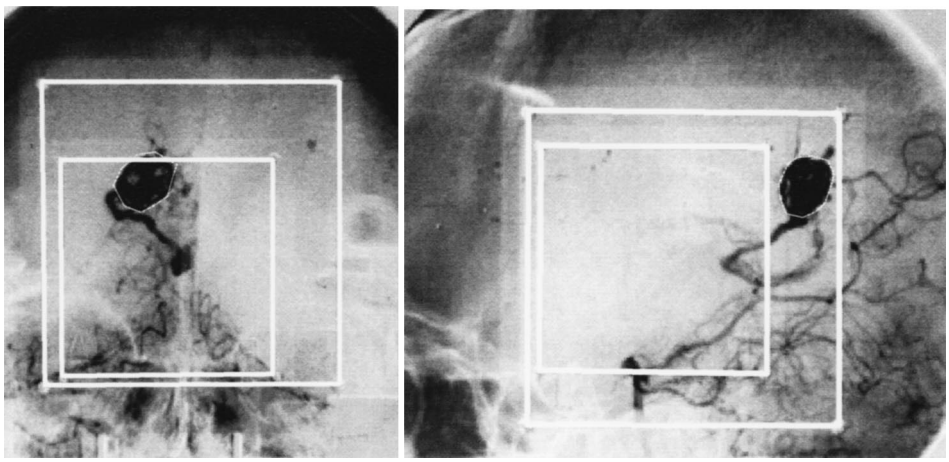

Fig. 5. Subtracted images of the frontal and lateral views from the angiography.

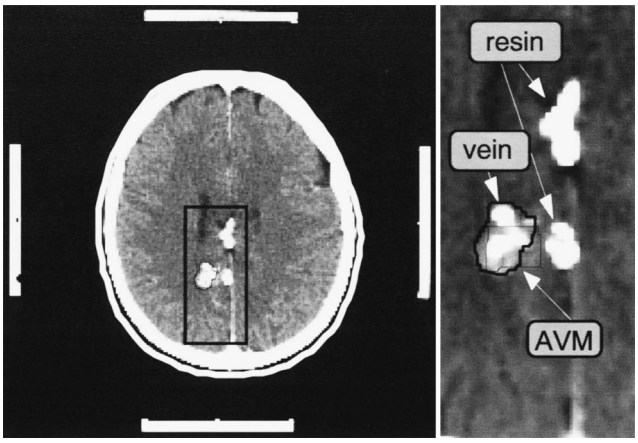

Fig. 6. CT image with administration of intravenous contrast medium. The shape in the thin line is calculated from the angiographic procedure. The contour in the bold line is drawn on the CT by the medical team.

evaluated by two incidences can be solved with our multi-incidence procedure.

2.2. Materials

The stereotactic equipment consists of a Riechert–Mundinger modified stereotactic head frame [19]. The patients are treated on a linear accelerator, Clinac 2100C (VARIAN), using additional collimators which produce circular beams having a diameter between 8 and 38 mm at the isocentre. The angiographic radiographs are taken using a magnification in the range of 1.1–1.7. The algorithm (written in C) runs on a DEC 5240 workstation using an ULTRIX 4.3 operating system. The software is integrated into a commercially available stereotactic treatment planning package (ARTEMIS [11]).

2.3. Clinical practice

The patient lies in the same position for angiography, CT and treatment. Several (two or more) series of radiographs are taken under stereotactic conditions. The co-ordinates of the markers and the target volume are outlined on each film using a digitizer. The position and envelope of the lesion are determined in the ring's co-ordinate system. Each calculated contour is displayed by the treatment planning system in the corresponding CT slice, enabling information to be compared from the two diagnostic modalities in the CT environment. In addition, a projection of the CT volume into the angiography geometry [7,20] can also be calculated (see Fig. 7).

3. Results

3.1. Phantom test

A dedicated phantom has been developed to check the accuracy of the method and to test the technique in the clinical environment. This phantom is made of a Teflon sphere (diameter 31 mm) inserted in a ($10 \times 10 \times 12$ cm) Plexiglas block. The block is fixed to the ring at mechanically precisely known co-ordinates. A CT examination and several radiographs were made under stereotactic conditions. Each experiment was carried out with six incident angles. All sources of X-rays were determined with a standard deviation of 5 mm along the principal X-ray beam axis and 0.5 mm perpendicular to this axis. Fig. 4 demonstrates the improvement in quality of the volume definition with increasing numbers of incidence (2, 3, 4, 5 and 6). If the contours on the film are digitized using tangential segments rather than chords, then the calculated volume contains the whole true target volume.

In a more quantitative approach, it is observed that the target volume in cubic centimetres, estimated by the algorithm, decreases with each additional incidence and reaches asymptotically towards the real volume (see values in Fig. 4). Of course, once the calculated volume is sufficiently similar to the real target volume, further improvement by adding more incidences cannot be expected.

The precision of the target localization can be verified by comparing the co-ordinates of the centre of gravity of the

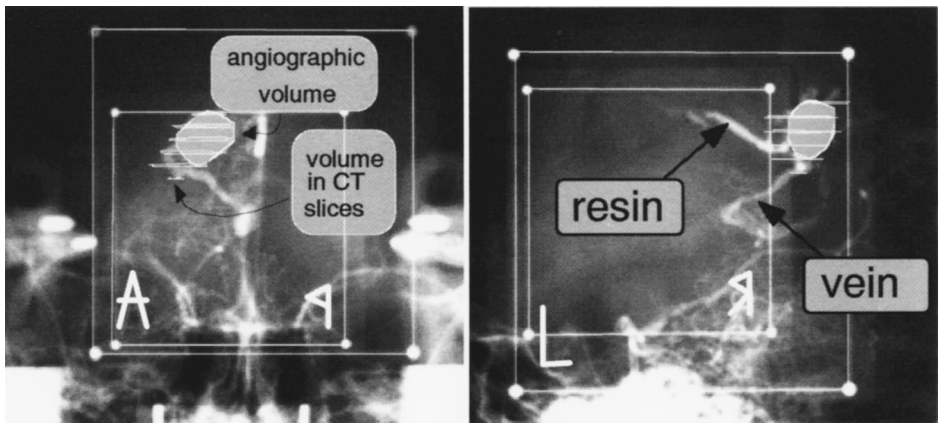

Fig. 7. CT contours seen in the angiographic geometry.

reconstructed volume with the centre of the real sphere. The distances between the centres were for 2, 3, 4, 5 and 6 incidences of 0.33, 0.38, 0.39, 0.38 and 0.26 mm, respectively. For all calculations, the agreement was within a 0.4 mm margin. Increasing the number of incidences cannot improve the results in this case because the target is symmetric and this implies that with two incidences the calculated centre of gravity is already according to the real one.

3.2. Clinical application

Following the phantom tests, the method was then applied to 11 patients. The procedure involves drawing the contours of the lesion (volume A) on the CT slices and then drawing the contours on the angiographic films (volume B). The two volumes can then be compared and the discussion will result in the final volume being corrected to correspond more precisely in both modalities.

To obtain an objective parameter describing the similarity of the two volumes (CT and angiography), a parameter of disagreement was introduced. This parameter can also be geometrically understood as a sort of distance. The volumes $A \cap B$ (intersection of A and B) and $A \cup B$ (combination of A and B) are calculated. The parameter of disagreement (d) is determined by:

$$d = 1 - \frac{\text{volume}(A \cap B)}{\text{volume}(A \cup B)} \quad (4)$$

where $d = 0$ means that the volumes A and B are identical and $d = 0.5$ means that the volume of $A \cap B$ is the same as the volume not common to A and B. If A and B are disconnected then $d = 1$.

The values of disagreement, d, for the 11 patients are given in Table 1. These are the values for the situation before comparison of images. They are sorted by disagreement parameter. For large volumes the agreement is better because the contouring on CT slices is much easier. In cases similar to the first case ($d = 0.27$), a better agreement could not really be expected because for geometric reasons the contour of the intersection resulting from the angiography volume (with only two incidences) with a CT slice resembles a quadrilateral (see the thin line in Fig. 6). The CT contours can be considered to be correct if the disagreement is smaller than 0.4, although they were always analyzed on images to improve the agreement. The last case ($d = 1$) was complicated due to the presence of resin. The volume on CT was mistaken with the resin. The technique described in this paper allows this type of misunderstanding to be avoided.

Table 1
Volumes and disagreements in 11 clinical cases

No.	Volume (cm^3)				Disagreement (d)
	Computed tomography	Angiography	Intersection	Union	
1	6.28	7.50	5.81	7.97	0.27
2	4.67	6.31	3.72	7.25	0.49
3	7.02	9.40	5.46	10.95	0.50
4	5.45	8.13	4.50	9.07	0.50
5	3.53	6.27	3.12	6.68	0.53
6	0.76	0.49	0.39	0.85	0.54
7	2.65	3.48	1.91	4.23	0.55
8	1.84	0.98	0.79	2.03	0.61
9	4.14	5.55	2.65	7.03	0.62
10	1.68	0.57	0.50	1.75	0.71
11	1.07	1.95	0.00	3.02	1.00

The disagreement parameter (d) calculated here is taken before the comparison of volumes. After the comparison, the disagreement is always smaller than 0.5. $d = 0$ means the volumes are the same and $d = 1$ means the volumes are not overlapping (the volume of the intersection is 0).

In order to illustrate in greater detail, case number 8 ($d = 0.61$) is presented. Fig. 5 shows the frontal and lateral view of the angiography. The nidus is outlined on these subtracted images. The AVM was delineated manually on the CT slice (see the bold line in Fig. 6) and the contour resulting from the angiography information was calculated by the described method. The contrasted resin stemming from a preceding embolization was indistinguishable from the target volume on the CT slice, but was excluded by the angiography.

Using a simple projection algorithm, it is possible to reproject the target of the enhanced CT into the angiography geometry (see Fig. 7). A significant difference is seen in the two volumes. In the CT approach, the outlined volume contains true nidus, resin on the arterial side (see lateral view in Fig. 7) and part of a large draining vein on the inferior part of the lesion (see frontal view in Fig. 7). The addition of angiographic information allows the size of the treatment field to be reduced from 21 to 18 mm at the isocentre and consequently results in the irradiated volume being reduced by about 40%.

4. Conclusion

Stereotactic radiosurgery for arteriovenous malformations requires a high precision in the delineation of the target volume. Imaging techniques such as CT and angiography are combined in order to obtain a better spatial resolution. CT data counterbalances the relative weakness of angiography as far as three-dimensional geometry is concerned. The angiography adds useful information to the CT especially concerning the arterial feeding, the venous drainage of the nidus and the presence of resin. The proposed method takes into account both modalities and reveals the discrepancy between the target locations defined by the CT and angiography. The possibility of identifying more complex lesion during the angiographic examination is one of the major advantages of this new technique. The increase in resolution for the characterization of the target is influenced by three factors, i.e. the increase in the number of incidences, the choice of the incidences and the use of convex sub-volumes

clearly identified on the angiography. Perhaps more important than the precision is the additional degree of safety supplied by the explicit comparison of volumes. Almost all the clinical cases presented here confirm the benefit of being able to compare both volumes.

References

[1] Bergström, M., Greitz, T. and Steiner, L. An approach to stereotaxic radiography. Acta Neurochir. 54: 157–165, 1980.

[2] Bergström, M., Greitz, T. and Ribble, T. A method of stereotaxic localization adopted for conventional and digital radiography. Neuroradiology 28: 100–104, 1986.

[3] Bova, F.J. and Friedman, W.A. Stereotactic angiography: an inadequate database for radiosurgery. Int. J. Radiat. Oncol. Biol. Phys. 20: 891–895, 1991.

[4] Chaney, E.L. Integrated data in planning therapeutic interventions, digital imaging. In: Med. Phys. Monograph No. 22, 1993 Summer School Proceedings, University of Virginia, Charlottesville, VA.

[5] Dean, E.M. Intracranial Stereotactic Radiotherapy – The Myths and Realities, pp. 107–109. Proceedings of the 7th Varian European Users Meeting, Montreux, 1993.

[6] Foroni, R., Gerosa, M., Pasqualin, A. et al. Shape recovery and volume calculation from biplane angiography in the stereotactic radiosurgical treatment of arteriovenous malformations. Int. J. Radiat. Oncol. Biol. Phys. 35: 565–577, 1996.

[7] Henri, C.J., Collins, D.L. and Peters, T.M. Multi-modality image integration for stereotactic surgical planning. Med. Phys. 18: 167–177, 1991.

[8] Kantor, G. Activity of radiosurgery and stereotactic radiotherapy, the SFRO survey, 1993, Bulletin du Cancer. Radiothérapie 81: 170–173, 1994.

[9] Larson, D.A., Bova, F., Eisert, D. et al. Current radiosurgery practice: results of an ASTRO survey. Int. J. Radiat. Oncol. Biol. Phys. 28: 523–526, 1994.

[10] Lefkopoulos, D., Schlienger, M., Touboul, E. et al. A 3D radiosurgical methodology for complex arteriovenous malformations. Radiother. Oncol. 28: 233–240, 1993.

[11] Lefkopoulos, D., Schlienger, M., Plazas, M.C., Merieenne, L., Dominique, C. and Laugier, A. 3-D dosimetry for radiosurgery of complex AVMs, pp. 254–257. Editors: S. Hukku and P.S. Iyer. Proceedings of the 10th International Conference on the Use of Computers in Radiation Therapy ICCR, Lucknow, 1990.

[12] Leksell, L. Cerebral radiosurgery I. Gamma thalamotomy in two cases of intractable pain. Acta Chir. Scand. 134: 585–595, 1968.

[13] Leksell, L. Stereotaxis and Radiosurgery. An Operative System. Charles C. Thomas, Springfield, IL, 1971.

[14] Lemieux, L., Jagoe, R., Fish, D.R., Kitchen, N.D. and Thomas, D.G.T. A patient-to-computed-tomography image registration method based on digitally reconstructed radiographs. Med. Phys. 21: 1749–1760, 1994.

[15] Lutz, W., Winston, K.R. and Maleki, N. A system for stereotactic radiosurgery with a linear accelerator. Med. Phys. 13: 611, 1986.

[16] Philips, M.H., Kessler, M., Chuang, F.Y. et al. Image correlation of MRI and CT in treatment planning for radiosurgery of intracranial vascular malformations. Int. J. Radiat. Oncol. Biol. Phys. 20: 881–889, 1991.

[17] Siddon, R.L. and Barth, N.H. Stereotactic localization of intracranial targets. Int. J. Radiat. Oncol. Biol. Phys. 13: 1241–1246, 1987.

[18] Spiegelmann, R., Friedman, W.A. and Bova, F.J. Limitations of angiographic target localization in planning radiosurgical treatment. Neurosurgery 30: 623–624, 1992.

[19] Sturm, V., Pastyr, O., Schlegel, W., Scharfenberg, H. et al. Stereotactic computer tomography with a modified Riechert–Mundinger device as the basis for integrated stereotactic neuroradiological investigations. Acta Neurochir. 68: 11–17, 1983.

[20] Vandermeulen, D., Suetens, P., Gybels, J. and Oosterlink, A. A new software package for the microcomputer based BRW stereotactic system; integrated stereoscopic views of CT data and angiograms. Soc. Photo-Optical Instrum. Engineers 593: 103–114, 1985.

[21] Webb, S. The Physics of 3D Radiation Therapy, pp. 135–171. Editors: R.F. Mould, C.G. Orton, J.A.E. Spaan and J.G. Webster. Institute of Physics Publishing, Bristol, PA, 1993.